arXiv:1009.3938v3 [hep-th] 14 Jan 2011

Excited Hexagon Wilson Loops for Strongly Coupled $\mathcal{N} = 4$ SYM

J. Bartels[a] **J. Kotanski**[a] **V. Schomerus**[b,c]

[a] *II. Institute Theoretical Physics,*
Hamburg University, Germany

[b] *DESY Theory Group,*
Hamburg, Germany

[c] *Department of Physics and Astronomy,*
UBC, Vancouver, Canada

E-mail: joachim.bartels@desy.de, jan.kotanski@desy.de,
volker.shomerus@desy.de

ABSTRACT: This work is devoted to the six-gluon scattering amplitude in strongly coupled $\mathcal{N} = 4$ supersymmetric Yang-Mills theory. At weak coupling, an appropriate high energy limit of the so-called remainder function, i.e. of the deviation from the BDS formula, may be understood in terms of the lowest eigenvalue of the BFKL hamiltonian. According to Alday et al., amplitudes in the strongly coupled theory can be constructed through an auxiliary 1-dimensional quantum system. We argue that certain excitations of this quantum system determine the Regge limit of the remainder function at strong coupling and we compute its precise value.

Contents

1 Introduction

The correspondence between $\mathcal{N} = 4$ supersymmetric Yang-Mills theory and string theory on an $AdS_5 \times S_5$ geometry is the most studied example of a gauge/string duality [1–4]. After the impressive progress that has been made in computing anomalous dimensions of gauge invariant operators, see e.g. [5–13] and references therein, the focus has recently shifted to the analysis of planar scattering amplitudes.

On the gauge theory side, the discussion was stimulated by the intriguing BDS formula of Bern, Dixon and Smirnov [14]. It encapsulates the known infrared and collinear behavior of n-particle maximally helicity violating (MHV) amplitudes in the planar approximation. The authors of [14] conjectured the BDS formula to determine the amplitudes at each loop order $L \geq 2$ up to some additive finite function $R^{(n)}$ of the kinematic variables. $R^{(n)}$ has been dubbed the 'remainder function'. Both string and gauge theory arguments suggest that the remainder function $R^{(n)}$ vanishes for $n = 4, 5$. In the weakly coupled theory, perturbative computations have uncovered an important new symmetry of scattering amplitudes [15]. Assuming this so-called *dual conformal symmetry*, the remainder functions

$R^{(n)}$ can only depend on conformal cross ratios, i.e. on conformal invariant combinations of the usual kinematic variables. Since there are no such cross ratios for $n = 4, 5$, the corresponding remainder functions have to be trivial. In other words, dual conformal invariance predicts that the BDS formula is exact for $n = 4, 5$ to all loop orders. This prediction was confirmed by a string theory computation of the leading term at strong coupling. We shall say a bit more about the string theoretic analysis below.

On the other hand, the remainder function $R^{(n)}$ is known to be non-zero for $n > 5$ and beyond one loop [16, 17]. A first explicit disagreement between the BDS formula and calculations of Yang-Mills scattering amplitudes in the leading logarithmic high energy approximation was pointed out in [18, 19]. This outcome has been confirmed by a numerical analysis of existing two-loop calculations for the six-point function [20].

The analysis in [18, 19] illustrates the importance of the high energy limit (Regge limit) which, in particular, exhibits much of the subtle analytic structure of multiparticle amplitudes. Let us briefly recapitulate the main results. There are three different kinematical regions which are of interest. In the usual 'physical region' all energies of the process are positive. The opposite case in which all energies are negative is referred to as the 'Euclidean region'. Most of the analysis we shall discuss in this work, however, deals with a third region that contains both positive and negative energies, see eq. (2.8) and Fig. 1 for a precise definition of this 'mixed region'. It is the mixed region that offers the clearest view on the discrepancy between the BDS formula and the existing high energy calculations of gluon amplitudes. In fact, the six-gluon scattering amplitude in the mixed region includes a Regge-cut contribution which cannot be reproduced from the BDS formula. For the physical regime, the failure of the BDS formula manifests itself in a violation of the Steinmann relation. No disagreement is visible in the Euclidean region.

These findings imply that the remainder function $R^{(6)}$ vanishes in the high energy limit of both the Euclidean and the physical region. Upon analytic continuation into the mixed region, however, the high energy limit should be nonzero and, in the leading logarithmic approximation, must coincide with the contribution given in [19]. This emphasizes the importance of the correct analytic structure. In a recent study [21], a convenient analytic expression [22] for the exact two-loop calculation of the six-point function [23, 24] was used to perform the relevant analytic continuation. The results are in full agreement with [19]. This settles the remainder function in the two-loop approximation, and it supports the all-order leading log generalization in [18, 19].

The leading logarithmic approximation in the mixed region exhibits an important feature. As a function of the energy variable s_2 (see Fig.1) the six-gluon amplitude Amp$'$ [1] contains a Regge cut term with a power-like behavior

$$\text{Amp}' \sim s_2^{-E_2}, \tag{1.1}$$

where the (negative-valued) exponent E_2 is the lowest eigenvalue of the BFKL color-octet Hamiltonian H_2 for a two-gluon system. This term is missing in the BDS-amplitude and

[1]The $'$ is placed on this amplitude to remind us the high energy limit is taken in the mixed rather than the physical region.

therefore should be connected with the remainder function $R^{(6)}$. The BFKL color-octet Hamiltonian coincides with the Hamiltonian of an integrable open spin chain [25]. Similar results hold for scattering amplitudes involving $n > 6$ gluons. In a processes $2 \to 2n$ there exist Regge cut contributions with up to n gluons and the corresponding spin chains consist of n spins. Hence, the weak coupled theory provides direct evidence for integrability in the high energy behavior of planar scattering amplitudes.

Having reviewed all these results from gauge theory it is natural to ask what string theory has to say about the high energy limit of the remainder function $R^{(6)}$. In order to understand how the issue can be addressed, we need to briefly sketch the development that was initiated by the work [26] of Alday and Maldacena. The main insight of this paper was to identify the leading strong coupling contribution to an n-gluon amplitude with the area A_n of some 2-dimensional surface S_n inside AdS_5. According to the prescription of [26], S_n ends on a piecewise light-like polygon in the boundary of AdS_5. The light-like segments of this polygon are given by momenta p_j of the external gluons. For $n = 4$ it is possible to find the surface explicitly and the resulting amplitude matches the prediction from the BDS formula. Constructing S_n for $n > 5$, however, turned out to be a rather difficult problem, at least for finite n and generic choice of the external momenta. The issue was resolved through a series of papers [27–29] in which the area of S_n is related to the free energy of some auxiliary quantum integrable system. More precisely, it was argued that A_n may be computed from a family of functions $Y_{s,j}$ with $s = 1, 2, 3$ and $j = 1, \ldots, n-5$. The latter can be determined by solving a set of coupled non-linear integral equations. Very similar mathematical structures are actually familiar from the study of *ground states* in 1-dimensional quantum integrable systems. Moreover, the functional A_n resembles expressions for the free energy of such systems.

We employ this auxiliary quantum integrable system to study the Regge limit of the remainder function $R^{(6)}$ at strong coupling. The non-linear integral equations for the Y-functions we have mentioned in the previous paragraph provide an explicit set of equations which enable us to take the high energy limit and to investigate the analytic continuation between the physical and the mixed region. As the main result, we determine the value of the exponent E_2 at strong coupling,

$$E_2 \;=\; \frac{\sqrt{\lambda}}{2\pi} \left(\sqrt{2} + \frac{1}{2} \log(3 + 2\sqrt{2}) \right) \quad . \tag{1.2}$$

In passing to the mixed regime, we need to analytically continue the parameters of the auxiliary quantum integrable system. This continuation leads to a new system of equations with additional terms. The structure of the new integral equations and the corresponding modifications of the relevant energy functional are again familiar from the theory of quantum integrable systems. In that context they are used to describe *excitations* of the system. Our formula for the value of E_2 at strong coupling assumes that we can perform the analytic continuation into the mixed regime within the parameter-space of the quantum integrable system and that the corresponding amplitude is given by the exponential of the energy functional, as in the Euclidean regime.

This paper is organized as follows. In section 2 we define the kinematic regions and the path of analytic continuation for the kinematic variables. Section 3 starts with a brief summary of relevant results from the work of Alday et. al. As a first exercise we then verify that the Regge limit of the remainder function $R^{(6)}$ vanishes in the physical regime (up to an irrelevant constant). Sections 4 and 5 contain the main part of our analysis. In these two sections we perform the analytic continuation, discuss the origin of the additional terms and calculate their contribution to the amplitude. For pedagogical reasons, we first illustrate the general arguments with a simpler example that is taken from the work [30, 31] of Dorey et al. The generalization to the system of Alday et al. is straightforward. Section 5 is devoted to the analysis of the resulting equations. With strong support from numerics we argue that the transition to the mixed regime is associated with the simplest kind of excitations in the auxiliary integrable system. Once this is established, the precise value of E_2 can be calculated analytically. A few technical details are contained in two appendices.

2   Multi-Regge kinematics of six-gluon amplitudes

We consider the scattering of six gluons with momenta $p_j, j = 1, \ldots, 6$ satisfying the on-shell condition $p_j^2 = 0$. From these momenta we can form Lorentz invariant combinations of the form

$$x_{ij}^2 \;=\; (p_{i+1} + \cdots + p_j)^2 \;. \tag{2.1}$$

Throughout this note we shall use the metric $\eta = diag(-, +, +, +)$. Furthermore, we extend the range of the index j on p_j to the integers with the periodicity condition $p_j \equiv p_{j+6}$. Due to momentum conservation the quantities x_{ij}^2 are symmetric in their indices, i.e. the obey $x_{ij}^2 = x_{ji}^2$. Six-point amplitudes of a 4-dimensional gauge theory depend on eight kinematical invariants. Hence, there exist many relations between the x_{ij}^2 we introduced above.

In the literature, six-point amplitudes are usually parametrized in terms of the following nine invariants, as shown schematically in figure 1,

$$
\begin{aligned}
s \;&=\; -x_{26}^2, \qquad s_1 \;=\; -x_{24}^2, \qquad s_2 \;=\; -x_{35}^2, \qquad s_3 \;=\; -x_{46}^2, \\
& \qquad\qquad t_1 \;=\; -x_{13}^2, \qquad t_2 \;=\; -x_{15}^2, \\
s_{345} \;&=\; -x_{25}^2, \qquad s_{234} = -x_{14}^2, \qquad s_{456} \;=\; -x_{36}^2 \;.
\end{aligned} \tag{2.2}
$$

Variables denoted by s or t are referred to as energies and momentum transfers, resp. In the Regge limit, energies are large (and can be positive or negative), whereas momentum transfer variables are negative and finite. As an example, a positive energy s implies the negative distance x_{26}^2. Since we have only eight independent variables, one of the above can be eliminated with the help of the Gram determinant, namely $\det([p_i \cdot p_j]_{i,j=1,\ldots,5}) = 0$. Since each of the products $[p_i \cdot p_j]$ may be expressed through the kinematical invariants defined in eqs. (2.2), we can use the Gram determinant relation to eliminate one of these nine invariants.

In the physical regime, all the 's-like' kinematical invariants are positive while the 't-like' variables are negative, i.e.

$$s, s_i, s_{456}, s_{345} > 0 \quad \text{and} \quad t_i, s_{234} < 0 \ . \tag{2.3}$$

Finite quantities in a theory with dual conformal invariance can only depend on cross-ratios. For a six-point amplitude, there are three independent conformal cross-ratios which are defined as

$$u_1 = \frac{x_{13}^2 x_{46}^2}{x_{14}^2 x_{36}^2} = \frac{t_1 s_3}{s_{234} s_{456}} , \quad u_2 = \frac{x_{24}^2 x_{51}^2}{x_{25}^2 x_{41}^2} = \frac{s_1 t_2}{s_{345} s_{234}} , \quad u_3 = \frac{x_{35}^2 x_{62}^2}{x_{36}^2 x_{52}^2} = \frac{s_2 s}{s_{456} s_{345}} . \tag{2.4}$$

For later use we have expressed them both in terms of the general kinematical invariants x_{ij} and in terms of the nine special invariants that were defined in eq. (2.2).

In the next section we shall look at the multi-Regge limit for six-point functions which, by definition, explores the regime

$$s \gg s_1, s_2, s_3 \gg -t_1, -t_2, -s_{234} \sim \text{fixed} . \tag{2.5}$$

The conformal cross-ratios are functions of the kinematical invariants and one can study there behavior in the Regge regime. It turns out that

$$u_1 \sim u_2 \sim 1 - u_3 \to 0 \tag{2.6}$$

vanish in the same order (see Appendix A). Hence, the leading asymptotics of any conformal invariant of the momenta p_i may be parametrized by the two quantities

$$\tilde{u}_1 = u_1/(1 - u_3) \quad \text{and} \quad \tilde{u}_2 = u_2/(1 - u_3) \ . \tag{2.7}$$

In this simple multi-Regge limit, the six gluon scattering amplitude actually agrees with the answer that is predicted by the BDS formula. This is because the limiting values $(u_1, u_2, u_3)_{\text{Regge}} = (0, 0, 1)$, corresponds to a special case of the collinear limit, namely $u_1 = 0$, $u_3 = 1 - u_2$ where $u_2 \to 0$. In the collinear limit, the six-point amplitude reduces a 5-point amplitude which is known to be BDS exact. Hence, the Regge limit (2.5) of the BDS formula for six gluons needs no corrections and therefore is of no further interest to us, at least for the moment.

As we have outlined in the introduction, however, there exists another Regge limit in which the BDS formula requires corrections, i.e. the remainder function does not vanish. Reaching this limiting regime requires to pass to a new kinematic region which is defined as

$$s, s_2 > 0 \quad \text{and} \quad s_1, s_3, s_{345} s_{456} < 0 , \ t_1, t_2, s_{234} < 0 \ . \tag{2.8}$$

In the corresponding multi-Regge limit all energy variables are much larger than the momentum transfer variables,

$$s \gg s_2, -s_1, -s_3 \gg -t_1, -t_2, -s_{234} \sim \text{fixed} . \tag{2.9}$$
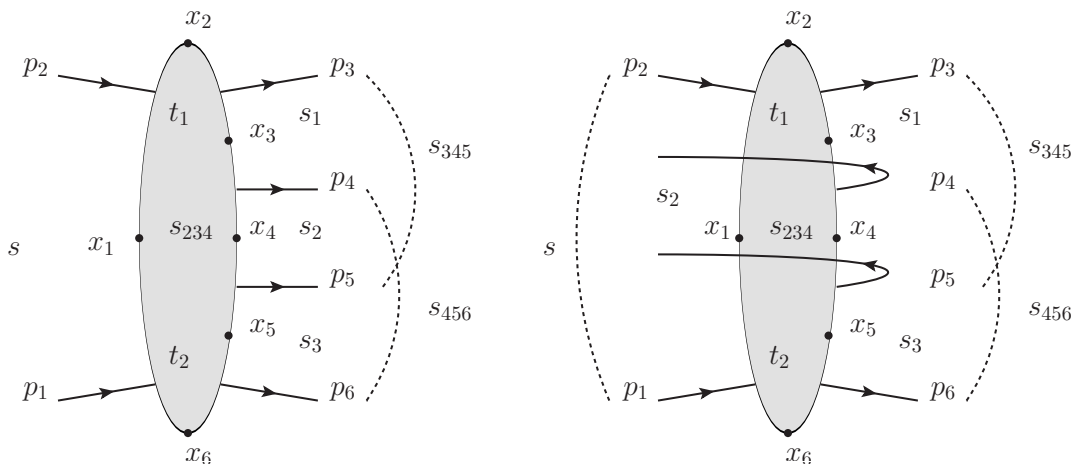
Figure 1. Kinematic configuration for the multi-Regge limit before (on the left) and after (on the right) the analytical continuation with the kinematic invariants from eq. (2.2). Momenta of are denoted by p_i while dual coordinates of the Wilson loop by x_i.

In order to reach this regime, one either starts from the region where all invariants are negative and then continues in s and s_2 or, alternatively, one first goes to the physical region and then continues all the following energy variables analytically along the following simple path

$$s_1(\varphi) = e^{i\varphi} s_1, \quad s_3(\varphi) = e^{i\varphi} s_3 \quad \text{and} \quad s_{456}(\varphi) = e^{i\varphi} s_{456}, \quad s_{345}(\varphi) = e^{i\varphi} s_{345},$$
(2.10)

where $\varphi \in [0, \pi]$ and all the other kinematical invariants are left unaltered. In the process of the continuation, the conformal cross ratios u_1 and u_2 are left invariant while u_3 behaves as

$$\mathcal{C}_u : \quad u_3(\varphi) = e^{-2i\varphi} u_3 .$$
(2.11)

At the final point $\varphi = \pi$ all three cross-ratios come back to their original values. Along the way, the cross-ratio u_3 moves along a full circle.

Our analysis below starts with some conformal amplitude $A(u_i)$ in the physical regime. Its precise form will be described in the next section. In a first step we want to continue this amplitude analytically along the path (2.11). Since $A(u_i)$ is not single valued in the complex u−space, the resulting amplitude $A^{\mathcal{C}}(u_i)$ differs from the amplitude we started with. Then we perform the Regge limit. This leaves us with a function $a(\tilde{u}_1, \tilde{u}_2)$ that describes the leading Regge asymptotics of $A^{\mathcal{C}}$. It is this quantity we are actually after.

The amplitude we shall subject to this analysis is taken from the recent work of Alday et al. By construction, it is initially defined in the Euclidean region in which all the kinematical invariants (2.2) are negative. In order to go to the physical region (2.3) one needs to continue s, s_i, s_{345} and s_{456} analytically while keeping t_i and s_{234} fixed. This continuation may be performed such that all three conformal cross-ratios u_i remain fixed.

Hence, conformal amplitudes do not require analytical continuation in order to pass from the Euclidean to the physical region.

3 Six gluon amplitudes at strong coupling

In the first part of this subsection, we shall briefly recall the prescription of Alday et al. for six gluon amplitudes at strong 't Hooft coupling. The second subsection contains an analysis of the Regge limit in the physical regime. We shall demonstrate that the Regge limit of the six gluon amplitude is BDS exact, in agreement with general arguments.

3.1 Review of results from Alday et al.

According to the work of Alday et al. [28], the strong coupling limit of a six gluon amplitude in $\mathcal{N} = 4$ supersymmetric Yang-Mills theory is obtained through exponentiation of the quantity

$$A^{(6)} = A^{(6)}_{\mathrm{div}} + A^{(6)}_{\mathrm{BDS\text{-}like}} + A^{(6)}_{\mathrm{free}} + A^{(6)}_{\mathrm{period}} , \tag{3.1}$$

at least up to a constant that is independent of the kinematics. The various pieces on the right hand side are all known explicitly. In particular the divergent contribution is given by

$$A^{(6)}_{\mathrm{div}} = \frac{1}{8} \sum_i \log^2(\epsilon^2 x^2_{i,i+2}) , \tag{3.2}$$

where ϵ is the cut-off. The BDS-like amplitude is also relatively simple. In the case of six gluon scattering, it is given by

$$A^{(6)}_{\mathrm{BDS\text{-}like}} = -\frac{1}{8} \sum_{i=1}^{6} \left(\log^2 x^2_{i,i+2} + \sum_{k=0}^{2} (-1)^{k+1} \log x^2_{i,i+2} \log x^2_{i+2k+1,i+2k+3} \right) . \tag{3.3}$$

For us, it is most relevant to have an expression for the difference between the usual BDS and the BDS-like amplitudes. This difference is given by

$$\Delta^{(6)} = A^{(6)}_{\mathrm{BDS}} - A^{(6)}_{\mathrm{BDS\text{-}like}} = \sum_{i=1}^{3} \left(\frac{1}{8} \log^2 u_i + \frac{1}{4} \mathrm{Li}_2(1 - u_i) \right) . \tag{3.4}$$

The conformal cross-ratios u_i that appear in this expression were defined in the previous section.

The two remaining contributions to the total amplitude cannot be written directly in terms of the three cross-ratios u_i. Instead, they involve a new set of parameters m, C, ϕ that are related to the u_i through some functional relations to be spelled out below. Given m, C, ϕ Alday et al. instruct us to solve the following system of non-linear integral equations for three functions $Y_i = Y_i(\theta), i = 1, 2, 3,$

$$\log Y_2(\theta) = -m\sqrt{2} \cosh(\theta - i\phi) - 2 \int_{-\infty}^{\infty} d\theta' K_1(\theta - \theta') \log(1 + Y_2(\theta'))$$

$$- \int_{-\infty}^{\infty} d\theta' K_2(\theta - \theta') \log((1 + Y_1(\theta'))(1 + Y_3(\theta'))) , \tag{3.5}$$

$$\log Y_{2\pm1}(\theta) = -m\cosh(\theta - i\phi) \pm C - \int_{-\infty}^{\infty} d\theta' K_2(\theta - \theta')\log(1 + Y_2(\theta'))$$
$$- \int_{-\infty}^{\infty} d\theta' K_1(\theta - \theta')\log((1 + Y_1(\theta'))(1 + Y_3(\theta'))) . \tag{3.6}$$

These formulas can be used as long as $|\operatorname{Im}(\theta - i\phi)| < \pi/2$. For values of θ outside this strip, one can employ certain recurrence relation to determine Y_i; details are given in the Appendix B. The equations (3.5) and (3.6) involve two integral kernels K_1 and K_2 that are given by

$$K_1(\theta) = \frac{1}{2\pi\cosh\theta} , \quad K_2(\theta) = \frac{\sqrt{2}\cosh\theta}{\pi\cosh 2\theta} . \tag{3.7}$$

Suppose for the moment that we can solve these equations somehow. The resulting functions $Y_i(\theta)$ clearly depend on the parameters m, C and ϕ in some complicated way. It is now possible to express m, C, ϕ through the cross ratios u_i by solving the following three equations

$$u_1 = \frac{x_{13}^2 x_{46}^2}{x_{14}^2 x_{36}^2} = \left(1 + \frac{1}{Y_2(\theta = -i\pi/4)}\right)^{-1} ,$$

$$u_2 = \frac{x_{24}^2 x_{15}^2}{x_{25}^2 x_{14}^2} = \left(1 + \frac{1}{Y_2(\theta = i\pi/4)}\right)^{-1} , \tag{3.8}$$

$$u_3 = \frac{x_{35}^2 x_{26}^2}{x_{36}^2 x_{25}^2} = \left(1 + \frac{1}{Y_2(\theta = -3i\pi/4)}\right)^{-1} .$$

The last equation contains the function Y_2 outside the strip $|Im(\theta - i\phi)| < \pi/2$. With the recurrence relations described in the Appendix B we rewrite this equation in the following form

$$u_3 = \left.\frac{(1 - u_2)u_2}{(1 + Y_1)u_2 + (u_2 + Y_1)Y_3}\right|_{\theta=0} = \left.\frac{(1 - u_1)u_1}{(1 + Y_1)u_1 + (u_1 + Y_1)Y_3}\right|_{\theta=0} . \tag{3.9}$$

Once $m = m(u_i), C = C(u_i)$ and $\phi = \phi(u_i)$ are known, we can construct the two missing terms of the total amplitude. The so-called free energy is given by

$$A_{\text{free}}^{(6)} = \int \frac{d\theta}{2\pi} m\cosh\theta\log\left[(1 + Y_1(\theta + i\phi))(1 + Y_3(\theta + i\phi))(1 + Y_2(\theta + i\phi))^{\sqrt{2}}\right] . \tag{3.10}$$

The final contribution to the amplitude depends on the cross ratios only through the parameter $m = m(u_i)$,

$$A_{\text{period}}^{(6)} = \frac{1}{4} m^2 . \tag{3.11}$$

This concludes our description of the input from the work of Alday et al.

3.2 Expansion for large masses

It is instructive to first study the Regge limit in the physical region and to verify that the remainder function does indeed vanish (up to a constant). Most of the formulas in this

subsection have appeared in the literature before, see [32, 33]. We repeat them here mostly for pedagogical reasons.

In the region (2.3) one can show that the multi-Regge limit is mapped onto large values of m, while C remains constant and ϕ goes to zero. To see this we start from eqs. (3.8), (3.9) and observe that our Regge limit (2.6) forces the values $Y_2(\pm i\pi/4)$, $Y_1(0)$, $Y_3(0)$ to approach zero at the same rate, i.e. the right hand sides of eqs. (3.5) and (3.6) must become large and negative. As long as $|\phi| < \pi/4$, the parameter m is forced to become large and the first terms on the right hand side dominate, i.e.

$$\log Y_2(\theta) \approx -m\sqrt{2}\cosh(\theta - i\phi)\,, \tag{3.12}$$

$$\log Y_{2\pm1}(\theta) \approx -m\cosh(\theta - i\phi) \pm C\,. \tag{3.13}$$

As we shall demonstrate further below, these approximations are justified since the integrals on the right hand side of eqs. (3.5) and (3.6) remain finite. This will no longer be that case after analytic continuation into the kinematic region (2.8). Taking the difference of the two equations (3.6) we obtain

$$Y_3(0)/Y_1(0) \;=\; e^{2C}\,. \tag{3.14}$$

As we argued above, the Regge limit requires both $Y_1(0)$ and $Y_3(0)$ to approach zero at the same rate so that their ratio stays fixed. Hence, in our Regge limit C is a finite constant. Finally, the ratio of u_1 and u_2, which should also be nonzero and finite in the Regge limit, is given by

$$u_1/u_2 \;\sim\; Y_2(\theta = -i\pi/4)/Y_2(\theta = i\pi/4) + \dots\,.$$

Here we have omitted terms of lower order in the Regge limit. Using eq. (3.12) we conclude that $m\sin\phi$ has to be finite, i.e. that ϕ tends to zero.

For the following analysis of the Regge limit it is convenient to introduce the parametrization

$$\varepsilon \;=\; e^{-m\cos\phi}\,,\quad w \;=\; e^{m\sin\phi}\,,\quad c \;=\; \cosh(C)\,. \tag{3.15}$$

We shall expand all equations from the previous subsection in the limit $\varepsilon \to 0$ while keeping both w and c fixed. From eqs. (3.8) we find that

$$u_1 = w\varepsilon + O\left(\varepsilon^2\right)\,,$$
$$u_2 = w^{-1}\varepsilon + O\left(\varepsilon^2\right)\,,$$
$$u_3 = 1 - (w + 2c + w^{-1})\varepsilon + O\left(\varepsilon^2\right)\,. \tag{3.16}$$

One easily verifies that the dependence of the conformal cross ratios on ε agrees with their behavior in the Regge limit, i.e. u_1, u_2 and $1 - u_3$ vanish in the same order, when ε is sent to zero. The leading contributions to all conformal invariants in the Regge limit are parametrized by the two functions

$$\tilde{u}_1 \;=\; \frac{u_1}{1 - u_3} \;\approx\; \frac{w^2}{w^2 + 2cw + 1}\,,\quad \tilde{u}_2 \;=\; \frac{u_2}{1 - u_3} \;\approx\; \frac{1}{w^2 + 2cw + 1}\,.$$

We can invert these two equations to determine w and c as functions of $\tilde{u}_1$ and $\tilde{u}_2$,

$$w(\tilde{u}_i) \approx \sqrt{\frac{\tilde{u}_1}{\tilde{u}_2}} , \quad c(\tilde{u}_i) \approx \frac{1 - \tilde{u}_1 - \tilde{u}_2}{2\sqrt{\tilde{u}_1\tilde{u}_2}} . \tag{3.17}$$

Our aim now is to evaluate the dependence of the so-called remainder function R,

$$-R^{(6)}(u_i) = A^{(6)} - A^{(6)}_{\text{div}} - A^{(6)}_{\text{BDS}} = A^{(6)}_{\text{free}} + A^{(6)}_{\text{period}} - \Delta^{(6)} + \text{constant} , \tag{3.18}$$

in the Regge limit as a function of $\tilde{u}_1$ and $\tilde{u}_2$. The function Δ was spelled out in eq. (3.4). In our limit we find that it is given by

$$-\Delta^{(6)} = A^{(6)}_{\text{BDS-like}} - A^{(6)}_{\text{BDS}} = -\sum_{i=1}^{3} \left(\frac{1}{8} \log^2 u_i + \frac{1}{4}\text{Li}_2(1 - u_i) \right)$$

$$= -\frac{1}{4} \log^2(w) - \frac{1}{4} \log^2(\varepsilon) - \frac{\pi^2}{12} + O(\varepsilon) . \tag{3.19}$$

The divergent contribution is actually cancelled exactly when we subtract the period contribution to the remainder function

$$A^{(6)}_{\text{period}} = \frac{1}{4} m^2 = \frac{1}{4} \log^2(w) + \frac{1}{4} \log^2(\varepsilon) . \tag{3.20}$$

It now remains to compute the contribution from the free energy to leading order in the Regge limit. When we send m to infinity, the functions Y_i become small all along the real axis so that we can approximate $\log(1 + Y_i(\theta)) \sim Y_i(\theta)$. In this limit, the free energy then takes the form

$$A^{(6)}_{\text{free}} \approx m \int \frac{d\theta}{2\pi} \cosh\theta\, Y_1(\theta + i\phi) + m \int \frac{d\theta}{2\pi} \cosh\theta\, Y_3(\theta + i\phi)$$

$$+\sqrt{2}m \int \frac{d\theta}{2\pi} \cosh\theta\, Y_2(\theta + i\phi) . \tag{3.21}$$

All three integrals can be evaluated easily with the help of the following integral formula

$$\int_{-\infty}^{\infty} \frac{d\theta}{2\pi} \cosh\theta\, e^{-am\cosh\theta} = \frac{1}{\pi} K_1(am) , \tag{3.22}$$

such that

$$A^{(6)}_{\text{free}} \approx \frac{2m}{\pi} \cosh(C) K_1(m) + \frac{\sqrt{2}m}{\pi} K_1(\sqrt{2}m) . \tag{3.23}$$

In the limit of large m we can use the asymptotic form of $xK_1(x) \sim \sqrt{\pi x/2} \exp(-x)$. Since the parameter m depends on ε through

$$m = \left(\log^2\varepsilon + \log^2 w\right)^{1/2} \approx -\log\varepsilon - \frac{1}{2}\frac{\log^2 w}{\log\epsilon} + \dots$$

we conclude that the free energy vanishes when ε is sent to zero. Indeed, once we insert the leading dependence of $m \sim -\log \varepsilon$ in ε into the formula (3.23) for the free energy, we obtain

$$A^{(6)}_{\text{free}} = \sqrt{\frac{2}{\pi}}\, c\, \varepsilon\, \sqrt{-\log \varepsilon} + \dots \,. \qquad (3.24)$$

where ... represent lower order terms. Combining this result with our previous equations (3.19), (3.20) and (3.24) for the Regge limit of the amplitude Δ and the periodic contribution we obtain,

$$- R^{(6)}(u_i) \approx -\tfrac{\pi^2}{12} + \text{constant} + O\left(\varepsilon\right) \,. \qquad (3.25)$$

As we had anticipated, the leading Regge asymptotics of the remainder function in the physical regime (2.3) is a constant.

4 Excited states in thermodynamic Bethe Ansatz

In this section we shall perform the analytic continuation of the kinematic variables along the path (2.10), and we show that excited states of the system start to contribute. To explain the basic ideas, we begin the presentation of a toy model [30, 31]. The corresponding analysis of the system (3.5) and (3.6) is more involved and is performed in the second subsection.

4.1 Analytical continuation and excited state TBA

As a warmup example we want to study a rather simple non-linear integral equation that depends on a single complex parameter m. We are interested in the behavior of the energy $F_0(m)$ as it is continued analytically in the parameter m. Our toy system involves a single function $Y(\theta)$ which is determined by

$$- \log Y(\theta) \;=\; m \cosh \theta - \frac{1}{2\pi} \int_{-\infty}^{\infty} K(\theta - \theta') \log \left(1 + Y(\theta')\right) \,. \qquad (4.1)$$

We shall think of the kernel function $K(\theta)$ as being determined through an S-matrix,

$$K(\theta) \;=\; -i\frac{\partial}{\partial \theta} \log S(\theta) \,. \qquad (4.2)$$

If the S-matrix is unitary, i.e. $S(\theta)S^{-1}(-\theta) = 1$, then the function $\log S(\theta)$ is antisymmetric and so $K(\theta)$ is invariant under $\theta \to -\theta$. Let us furthermore assume that the ground state free energy is given by

$$F_0(m) \;=\; \frac{3}{\pi^2} \int_{-\infty}^{\infty} d\theta\, m \cosh \theta \log \left(1 + Y(\theta)\right). \qquad (4.3)$$

In order to understand how $F_0(m)$ depends on the mass, it is quite instructive to study a trivial system with constant S-matrix. In this case, the equation (4.1) determines the

solution $\log Y(\theta) = -m \cosh \theta$ and we can evaluate the free energy of the ground states exactly,

$$
F_0(m) = \frac{3}{\pi^2} \int_{-\infty}^{\infty} d\theta \, m \cosh \theta \log(1 + e^{-m \cosh \theta}) = \frac{6m}{\pi^2} \sum_{k=1}^{\infty} \frac{(-1)^{k-1}}{k} K_1(km)
$$

$$
= \frac{1}{2} - \frac{3m^2}{2\pi^2} \left[-\log m + \frac{1}{2} + \log \pi - \gamma_E \right]
$$

$$
+ \frac{6}{\pi} \sum_{k=1}^{\infty} \left(\sqrt{m^2 + (2k-1)^2 \pi^2} - (2k-1)\pi - \frac{m^2}{2(2k-1)\pi} \right) . \tag{4.4}
$$

with the Euler-Mascheroni constant $\gamma_E = \lim_{s \to \infty} (\sum_{m=1}^{\infty} m^{-1} - \log s) = 0.577215...$. The branch cut of the logarithm is chosen to lie along the negative imaginary axis. For the integration we have used formula (8.526) from [34]. Then we expressed the infinite sum over Bessel functions K_1 through simpler functions with the help of

$$
\sum_{k=1}^{\infty} K_0(kx) = \frac{1}{2}(\gamma_E + \log \tfrac{x}{4\pi}) + \pi \sum_{k=1}^{\infty} \left[\frac{1}{\sqrt{x^2 + (2k-1)^2 \pi^2}} - \frac{1}{2k\pi} \right] . \tag{4.5}
$$

In addition, we used the formula $[xK_1(x)]' = -xK_0(x)$ for the derivative of $xK_1(x)$. The free energy $F_0(m)$ possesses a series of square root singularities at the points $x_k = i(2k-1)\pi$. Upon analytical continuation along a curve $\mathcal{C}$ that encircles the first N of these singularities in the upper half of the complex plane, we obtain

$$
F_0^{\mathcal{C}}(m) = F_0(m) - \frac{12}{\pi} \sum_{k=1}^{N} \sqrt{m^2 + (2k-1)^2 \pi^2} . \tag{4.6}
$$

We shall reproduce this simple answer down below through an analysis that does not require the S-matrix to be trivial.

When the system possesses a non-trivial S-matrix, the free energy can no longer be evaluated exactly. Nevertheless, we can still analyse how the the free energy $F_0(m)$ changes under analytic continuation in the mass parameter m. We begin by re-writing our non-linear integral equation (4.1) in the form

$$
-\log Y(\theta) = m \cosh \theta - \frac{1}{2\pi} \int_{-\infty}^{\infty} d\theta' (-i \frac{\partial}{\partial \theta} \log S(\theta - \theta')) \log(1 + Y(\theta'))
$$

$$
= m \cosh \theta + \frac{1}{2\pi} \int_{-\infty}^{\infty} d\theta' i \log S(\theta - \theta') \frac{Y'(\theta')}{1 + Y(\theta')} . \tag{4.7}
$$

Note that the integrand has poles at those points θ_0 at which the solution $Y(\theta)$ assumes the value $Y(\theta_0) = -1$. Since the solutions $Y(\theta)$ depend on the parameter m, the solutions of $Y(\theta_0) = -1$ depend on m, i.e. they move through the complex plane as we vary the parameter m. Whenever one of these solutions approaches the integration contour, we deform it so that solutions never cross. We do that until we get back to the original value of m. At this point we now determine a solution $Y^{\mathcal{C}}(\theta)$ through an equation of the same

form as eq. (4.1) but along some oddly shaped contour that depends on $\mathcal{C}$. We want to move the contour back to the real axis. Along the way we pick up contributions from the solutions of the equations

$$Y^{\mathcal{C}}(\theta_i) = -1 . \qquad (4.8)$$

Once the integration contour is back on the real axis, our non-linear integral equation takes the form

$$-\log Y^{\mathcal{C}}(\theta) = m \cosh \theta - \frac{1}{2\pi} \int_{-\infty}^{\infty} d\theta' K(\theta - \theta') \log(1 + Y^{\mathcal{C}}(\theta')) - \sum_{i=1}^{N} (-1)^{n_i} \log S(\theta - \theta_i), \qquad (4.9)$$

with integers n_i depending on the contour. The two equations (4.8) and (4.9) determine the function $Y^{\mathcal{C}}$ along with the parameters θ_i. Similarly, from the following formula for the free energy

$$F_0(m) = \frac{3}{\pi^2} \int_{-\infty}^{\infty} d\theta \, m \cosh \theta \log(1 + Y(\theta)) = -\frac{3}{\pi^2} \int_{-\infty}^{\infty} d\theta \, m \sinh \theta \frac{Y'(\theta)}{1 + Y(\theta)} . \qquad (4.10)$$

we infer that

$$F_0^{\mathcal{C}}(m) = \frac{3}{\pi^2} \int_{-\infty}^{\infty} d\theta \, m \cosh \theta \log(1 + Y^{\mathcal{C}}(\theta)) - \frac{6m}{\pi} \sum_{i=1}^{N} (-1)^{n_i} i \sinh \theta_i . \qquad (4.11)$$

In order to compare with our previous result (4.6) for the trivial system, we set $S = 1$ so that $-\log Y^{\mathcal{C}} = -\log Y = m \cosh \theta$. Suppose that m is continued along a curve in the upper half of the complex m-plane that encircles the points $m = i\pi(2k-1)$ for $k = 1, \ldots, N$. Then there are $2N$ solutions of the equation $Y(\theta) = -1$ that cross the real line. Since these are located at $\pm\theta_k$ with $m \cosh \theta_k = \pm i(2k-1)\pi$, formula (4.11) becomes

$$F_0^{\mathcal{C}}(m) = F_0(m) - \frac{12m}{\pi} \sum_{k=1}^{N} i \sinh \theta_k = F_0(m) - \frac{12}{\pi} \sum_{k=1}^{N} \sqrt{(2k-1)^2 \pi^2 + m^2} .$$

Here, we expressed $\sinh \theta_k$ through $\cosh \theta_k$. The sum extends over N pairs of solutions $\pm\theta_k$. Note that both solutions within each pair contribute the same amount. Therefore, we have simply multiplied the sum over N terms by an overall factor of two. Our result is identical to our previous formula for F_0 in a trivial system.

We conclude our analysis of the toy model with a few important comments. The simplest non-trivial case of a continuation occurs when a single pair $\pm\theta_0$ of solutions to $Y(\theta_0) = -1$ crosses the real axis. In that case, our equations for $Y^{\mathcal{C}}, F_0^{\mathcal{C}}$ and θ_0 become

$$-\log Y^{\mathcal{C}}(\theta) = m \cosh \theta + \log \frac{S(\theta - \theta_0)}{S(\theta + \theta_0)} - \frac{1}{2\pi} \int_{-\infty}^{\infty} d\theta' K(\theta - \theta') \log(1 + Y^{\mathcal{C}}(\theta')) \quad (4.12)$$

$$F_0^{\mathcal{C}}(m) = \frac{12m}{\pi} i \sinh \theta_0 + \frac{3}{\pi^2} \int_{-\infty}^{\infty} d\theta \, m \cosh \theta \log(1 + Y^{\mathcal{C}}(\theta)) . \qquad (4.13)$$

The position of the θ_0 can be calculated making use of

$$-\log Y^{\mathcal{C}}(\theta_0) = i(2k-1)\pi = m \cosh \theta_0 - \log S(2\theta_0) + \log S(0)$$

$$-\frac{1}{2\pi} \int_{-\infty}^{\infty} d\theta' K(\theta_0 - \theta') \log(1 + Y^{\mathcal{C}}(\theta')) . \qquad (4.14)$$

The first equality is obtained from eq. (4.8) by taking the logarithm. The second equality just repeats the functional equation for $Y^{\mathcal{C}}$. According to the previous equation, the right hand side has to stay finite when we send the mass parameter m to infinity. Since the first term on the right hand side diverges with m, this divergence must be cancelled by one of the other terms.[2] In the limit $m \to \infty$, the integral is a small correction and $S(0)$ does not depend on m at all. Hence, the term $\log S(\theta_0)$ has to diverge with m, i.e. the parameter $2\theta_0$ has to approach one of the poles θ_S of the bare S-matrix. As we go to finite values of the mass parameter, this value of θ_0 will receive corrections,

$$\theta_0 = \theta_S/2 + \delta . \tag{4.15}$$

In principle, we can compute such corrections perturbatively in the mass parameter m. It will turn out later that the case of two poles crossing the real line is particularly relevant to the study of the Regge limit.

Before we return to the study of the equations (3.5) and (3.6), let us make one comment on the path of the analytic continuation. In this subsection we assumed the curve $\mathcal{C}$ to be closed in the complex m-plane, i.e. in the parameter space of the non-linear integral equation. This is important for the relation with excited states where m plays the role of a physical mass parameter. Our derivations, on the other hand, remain perfectly valid for arbitrary curves $\mathcal{C}$ that begin at m and end at a possibly different point m' of the m-plane. All we have to do is to replace m by m' in our equation (4.9) and all equations after eq. (4.11). This extension shall play an important role in the subsequent analysis.

4.2 Excited state TBA for six gluon amplitudes

It is not difficult to extend the analysis of the previous subsection to the system that describes scattering amplitudes of six gluons. In this case, we need to solve the equations (3.5) and (3.6) for three functions $Y_i, i = 1, 2, 3$. The form of these equations is very similar to eq. (4.1), with one notable difference. In the context of six-gluon amplitudes the physical parameters are the cross ratios u_i rather than the parameters m, C, ϕ. Since these two sets of variables are related by some non-linear equations (3.8), an open curve in the space of parameters m, C and ϕ may be mapped to a closed curve in the cross ratios. Consequently, we shall allow our curve $\mathcal{C}$ to end in a point m', C' and ϕ' that may differ from starting point m, C and ϕ. Dealing with the requirement $u'_i = u_i$ is differed to the next section.

When we analyzed our toy model is was crucial that the kernel function K could be obtained from an S-matrix through equation (4.2). In complete analogy, we need to find unitary, crossing symmetric S-matrices

$$\frac{\partial}{\partial \theta} \log S_j(\theta) = -2\pi i K_j(\theta) , \tag{4.16}$$

for the two kernels K_1 and K_2 that were defined in equation (3.7). The solution is given by

$$S_1(\theta) = i\frac{1 - ie^\theta}{1 + ie^\theta} , \quad S_2(\theta) = \frac{2i\sinh(\theta) - \sqrt{2}}{2i\sinh(\theta) + \sqrt{2}} . \tag{4.17}$$

---

[2]Here we assume that the solution of eq. (4.8) does not coincide with the zeroes of $\cosh\theta_0$. This holds true for the cases to be considered in the next section.

Up to a common sign, the solution is uniquely fixed by the unitarity condition

$$S(\theta)S(-\theta) \; = \; S(\theta)S^\star(\theta^*) \; = \; 1 \, . \tag{4.18}$$

One may also verify that S_i are crossing symmetric, i.e. that they obey

$$\bar{S}_j(\theta) \; = \; S_{a\bar{b}}(\theta) \; = \; S_{ab}(i\pi - \theta) \; = \; S_j(i\pi - \theta) \, , \tag{4.19}$$

where $\bar{S}_2(\theta) = S_2(\theta)$ and $\bar{S}_1(\theta) = -S_1(\theta)$. Once we have rewritten the functional equations in (3.5) and (3.6) in terms of S_i, we can perform a partial integration and analyze the behavior of solutions Y_i upon analytic continuation of the parameters m, C and ϕ. The results are

$$-\log Y_2^{\mathcal{C}}(\theta) = -m'\sqrt{2}\cosh(\theta - i\phi') - 2\int_{-\infty}^{\infty} d\theta' K_1(\theta - \theta')\log(1 + Y_2^{\mathcal{C}}(\theta'))$$

$$- \int_{-\infty}^{\infty} d\theta' K_2(\theta - \theta')\log((1 + Y_1^{\mathcal{C}}(\theta'))(1 + Y_3^{\mathcal{C}}(\theta'))) + \sum_{j=1}^{N_1}(-1)^{n_{1,j}}\log S_2(\theta - \theta_{1,j})$$

$$-2\sum_{j=1}^{N_2}(-1)^{n_{2,j}}\log S_1(\theta - \theta_{2,j}) - \sum_{j=1}^{N_3}(-1)^{n_{3,j}}\log S_2(\theta - \theta_{3,j}) \, , \tag{4.20}$$

and similarly

$$-\log Y_{2\pm1}^{\mathcal{C}}(\theta) = -m'\cosh(\theta - i\phi') \pm C' - \int_{-\infty}^{\infty} d\theta' K_2(\theta - \theta')\log(1 + Y_2^{\mathcal{C}}(\theta'))$$

$$- \int_{-\infty}^{\infty} d\theta' K_1(\theta - \theta')\log((1 + Y_1^{\mathcal{C}}(\theta'))(1 + Y_3^{\mathcal{C}}(\theta'))) - \sum_{j=1}^{N_1}(-1)^{n_{1,j}}\log S_1(\theta - \theta_{1,j})$$

$$-\sum_{j=1}^{N_2}(-1)^{n_{2,j}}\log S_2(\theta - \theta_{2,j}) - \sum_{j=1}^{N_3}(-1)^{n_{3,j}}\log S_1(\theta - \theta_{3,j}) \, , \tag{4.21}$$

with integers N_s and $n_{s,j}$ depending on the path of the analytical continuation. The parameters $\theta_{s,j}$ are obtained by solving the equations

$$Y_s^{\mathcal{C}}(\theta_{s,j}) \; = \; -1 \quad . \tag{4.22}$$

As before, we can now evaluate the formulas (4.20) and (4.21) at the points $\theta_{s,j}$ and insert the conditions

$$-\log Y_s^{\mathcal{C}}(\theta_{s,j}) \; = \; i(2k_{s,j} - 1)\pi \tag{4.23}$$

to obtain equations for the positions $\theta_{s,j}$. Since the resulting expressions are rather lengthy, we shall refrain from spelling them out. Similarly to the toy model considered in the previous subsection, the position to the nearest poles in the limit of large m are related to poles of the S-matrices S_j. Eqs. (4.23) and (4.21), for example, require that for every i at least one of the differences $\theta_{1,i} - \theta_{2\pm1,j}$ or $\theta_{1,i} - \theta_{2,j}$ must approach a pole of S_1 or S_2, respectively.

The role of the free energy F_0 is played by the functional $A_{\text{free}}^{(6)}$ that was defined in eq. (3.10). During the analytical continuation, this quantity changes according to

$$A_{free}^{(6),\mathcal{C}} = \int \frac{d\theta}{2\pi} m' \cosh\theta \log\left[(1 + Y_1^{\mathcal{C}}(\theta + i\phi'))(1 + Y_3^{\mathcal{C}}(\theta + i\phi'))(1 + Y_2^{\mathcal{C}}(\theta + i\phi'))^{\sqrt{2}}\right]$$

$$-m'i\sum_{j=1}^{\tilde{N}_1}(-1)^{\tilde{n}_{1,j}}\sinh\tilde{\theta}_{1,j} - m'i\sum_{j=1}^{\tilde{N}_3}(-1)^{\tilde{n}_{3,j}}\sinh\tilde{\theta}_{3,j} - \sqrt{2}m'i\sum_{j=1}^{\tilde{N}_2}(-1)^{\tilde{n}_{2,j}}\sinh\tilde{\theta}_{2,j}, \quad (4.24)$$

where variables $\tilde{\theta}_{s,j}$ stand for $\tilde{\theta}_{s,j} = \theta_{s,j} - i\phi'$. The possible $\theta_{s,j}$ that contribute terms to the second line are solutions of eq. (4.23) that have passed the line $\text{Im}\,\theta = -\phi$ upon analytic continuation. For nonzero ϕ, the number of such solutions and the direction in which they cross the line may differ from the corresponding numbers and directions for the real line $\text{Im}\,\theta = 0$. This is why we had to use new integers $\tilde{N}_s$ and $\tilde{n}_{s,j}$ instead of the corresponding parameters N_s and $n_{s,j}$ that appeared in the integral equations (4.20) and (4.21). With these comments we conclude our general discussion of analytic continuations in the parameters for six gluon scattering. We shall now return to the Regge limit.

5 Regge limit of six gluon amplitude

Now we are prepared to combine the results of the previous sections in order to complete our main goal, namely to determine the Regge limit of the six gluon amplitude in the regime (2.8). As explained in section 2, the first step involves an analytic continuation in u-space. The transformations (3.8) describe m, C, ϕ as a function of the conformal cross ratios u_i and hence they determine how the parameters of the integral equations (3.5) and (3.6) change under analytic continuations along $\mathcal{C}_u$. Some important features of the curve in the space of parameters m, C, ϕ are discussed in the first subsection. Numerical results show that very few solutions of the equations (4.22) actually cross the real line while we continue from the physical to the mixed regime. This enables us to determine an explicit formula for the Regge limit of the six gluon amplitude in the regime (2.8).

5.1 The path of the analytical continuation

Our first aim is to describe the path of the analytical continuation. As we explained in section 2, we would like to continue analytically along the path $\mathcal{C}_u$ that was defined in eq. (2.11) with u_1 and u_2 kept fixed. From the first two relations in eq. (3.8) we infer that

$$Y_2^- \stackrel{\text{def}}{=} Y_2(-i\pi/4) = \frac{u_1}{1 - u_1}, \quad Y_2^+ \stackrel{\text{def}}{=} Y_2(i\pi/4) = \frac{u_2}{1 - u_2}. \quad (5.1)$$

Note that the left hand side depends on the parameters m, C, ϕ which enter the nonlinear integral equations for Y_i. Since we want to keep the right hand side fixed, eqs. (5.1) provide two constraints on the form of the curve in the space of parameters m, C, ϕ.

We still need to explore one more relation that involves the cross ratio u_3. Let us recall that u_3 has been expressed in eq. (3.9) through the values of the functions Y_i in the strip
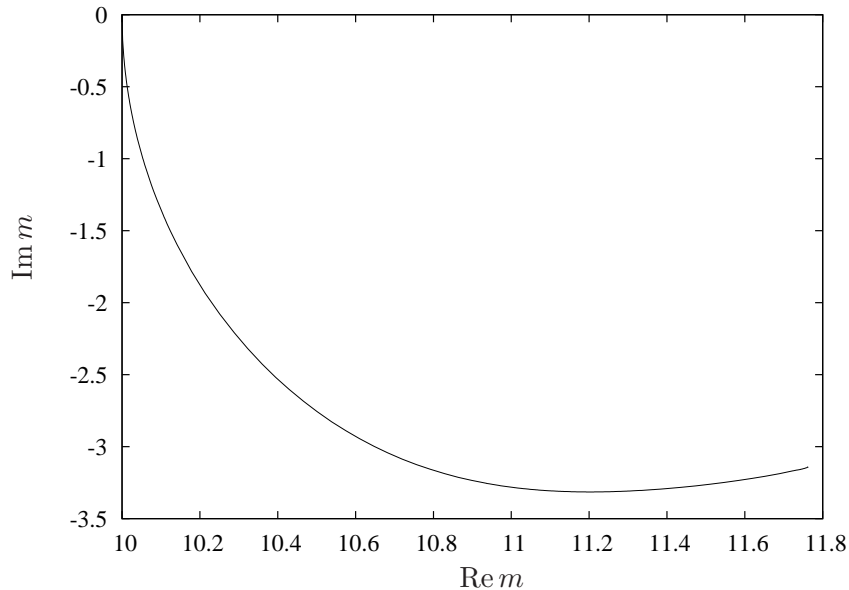
Figure 2. Upon analytic continuation along $\mathcal{C}$, the parameter m is shifted from its initial value. The plot shows numerical results for $m = 10$, $\cosh C = 3/5$ and $\phi = 0$ at $\varphi = 0$. Plots for different values of the parameter $C(\varphi = 0)$ differ by terms of order $\exp(-m)$.

$|Im(\theta - i\phi)| < \pi/2$. We can actually turn eq. (3.9) into a formula for $C = C(u_i)$ once we notice that

$$Y_3(\theta)/Y_1(\theta) \;=\; Y_3(0)/Y_1(0) \;=\; e^{2C} \;. \tag{5.2}$$

This simple relation follows by subtracting the non-linear integral equations (3.6) for Y_1 and Y_3 from each other. We employ eq. (5.2) to eliminate both Y_3 and Y_1 from the equation for u_3 and arrive at,

$$\cosh^2 C \;=\; \frac{(1 - u_1 - u_2 - u_3)^2}{4u_1 u_2 u_3} \;. \tag{5.3}$$

During our continuation we keep u_1 and u_2 fixed while u_3 is moved along a full circle until it comes back to its original position. Because the left hand side involves the square of $c = \cosh C$, the quantity $\cosh C$ has changed its sign once we reach the end-point of the curve $\mathcal{C}_u$. Note that eq. (5.3) determines the parameter C explicitly as a function of the cross ratios. The variation of the real and imaginary part of C along the path $\mathcal{C}_u$ is plotted in fig. 3. All the curves start in the lower half on the left hand side and proceed to the central line at $Im C = \pi/2$ and return to the left and into the upper half of the figure. At $\varphi = \pi/2$, the real part of C is of order m.

The dependence of m and ϕ on φ is a little more difficult to obtain. It requires inverting the eqs. (5.1) which contain the function Y_2. The latter must be determined numerically by solving the non-linear integral equation for a large number of values m, ϕ and C. Given u_i we can restrict the values of C to

$$\cosh^2 C(\varphi) \;=\; \frac{(1 - u_1 - u_2 - u_3 e^{-2i\varphi})^2}{4u_1 u_2 u_3 e^{-2i\varphi}} \;,$$
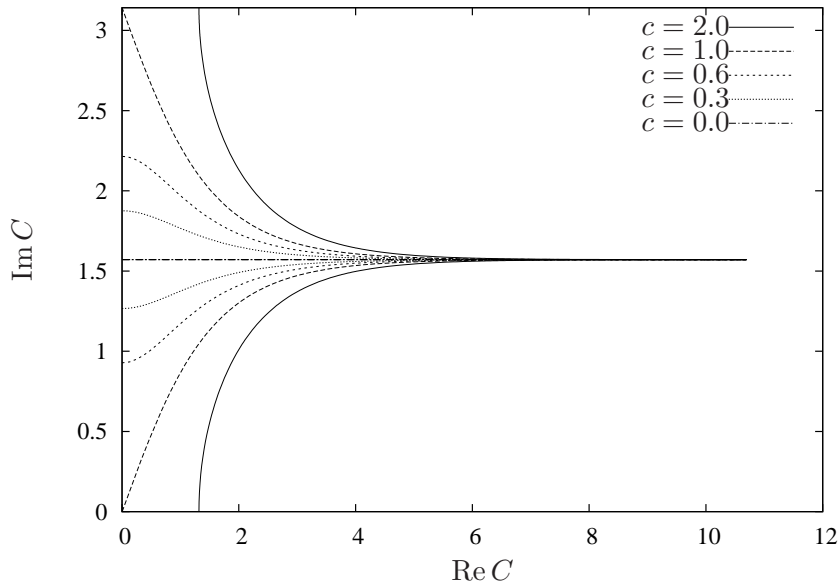
Figure 3. The plot shows the dependence of C on φ. The various curves correspond to the values $m = 10$, $\phi = 0$ and $\cosh C = c$ at the starting point $\varphi = 0$. Here, we plot C in its complex plane along the path given by (5.3) while $\phi(\varphi) = 0$.

where φ runs from $\varphi = 0$ to $\varphi = \pi$. We have performed these numerical studies for special cases in which $u_1 = u_2$. The condition amounts to setting $\phi = 0$ at $\varphi = 0$. It is not difficult to see that $\phi = 0$ will remain true as we move along the contour $\mathcal{C}_u$. Hence, it remains to determine $m(\varphi)$ such that $Y_2(\pm i\pi/4)$, and hence the cross ratios $u_1 = u_2$, remain invariant as me change φ. An example is shown in fig. 2. The shape of the curve has very little dependence on the parameter C. We observe that the parameter m becomes complex. At $\varphi = \pi$, its imaginary part is $\operatorname{Im} m(\pi) = -\pi$. The real part also gets shifted by an amount $\Delta m = \operatorname{Re} m(\pi) - \operatorname{Re} m(0) \sim 1.8$. We shall reproduce these shifts through an analytical argument in the next section. Some more comments on the numerical studies can be found in appendix C.

5.2 Evaluation of the Regge limit

In the previous section we have investigated the image of curve $\mathcal{C}_u$ in the space of parameters m, ϕ and C. For $\phi = 0$, the corresponding values of $m(\varphi)$ and $C(\varphi)$ are depicted in figs. 2 and 3. These numerical data provide us with a good qualitative understanding of the curve along which we would like to continue the parameters of the non-linear integral equations (3.5) and (3.6). As we discussed in section 4, we need to watch the solutions of $Y_i(\theta) = -1$ while continuing m, ϕ and C. Our numerical calculations show that, for large values of m, very few poles get close to the integration contour. In the case of Y_3, the numerical results are displayed in fig. 4. The plot was produced for a continuation along the paths described by figs. 2 and 3. We see a single pair of poles that crosses the real line. The symmetry under reflection $\theta \to -\theta$ is a direct consequence of our special choice $\phi = 0$.

Analogous results for the solutions of $Y_2 = -1$ are displayed in fig. 5. In this case, one pair of solutions approaches the real line while all others stay away from it. We did not display the corresponding plot for Y_1 since it looks very similar to that for Y_3, except for an overall shift by $\pm i\pi$.

With these results in mind we can actually spell out a system of equations that should determine the solutions Y_i at the end of the analytic continuation, i.e. in the mixed regime,

$$-\log Y_2'(\theta) = -m'\sqrt{2}\cosh(\theta - i\phi') - \int_{-\infty}^{\infty} d\theta' K_2(\theta - \theta')\log((1 + Y_1'(\theta'))(1 + Y_3'(\theta')))$$

$$-2\int_{-\infty}^{\infty} d\theta' K_1(\theta - \theta')\log(1 + Y_2'(\theta')) + \log S_2(\theta - \theta_1) - \log S_2(\theta - \theta_2), \quad (5.4)$$

$$-\log Y_{2\pm1}'(\theta) = -m'\cosh(\theta - i\phi') \pm C' - \int_{-\infty}^{\infty} d\theta' K_1(\theta - \theta')\log((1 + Y_1'(\theta'))(1 + Y_3'(\theta')))$$

$$-\int_{-\infty}^{\infty} d\theta' K_2(\theta - \theta')\log(1 + Y_2'(\theta')) + \log S_1(\theta - \theta_1) - \log S_1(\theta - \theta_2). \quad (5.5)$$

One might have expected to see additional terms from the solutions of $Y_2 = -1$ on the right hand side. As one may easily see, these take the form

$$\lim_{a \to 0} (2\log(S_1(\theta - a)) - 2\log(S_1(\theta + a))) = \lim_{a \to 0} (4i \operatorname{sech}(\theta)a) = 0, \quad (5.6)$$

and

$$\lim_{a \to 0} (2\log(S_2(\theta - a)) - 2\log(S_2(\theta + a))) = \lim_{a \to 0} \left(8i\sqrt{2}\cosh(\theta)\operatorname{sech}(2\theta)a\right) = 0. \quad (5.7)$$

Hence, we there are no additional terms on the right hand side of eqs. (5.4) and (5.5). In the above equations and throughout the entire discussion below we place a $\prime$ on all quantities that have been continued to the endpoint of the curve $\mathcal{C} = \mathcal{C}_u$ that we described in the previous subsection. The parameters θ_1 and θ_2 appearing in the arguments of the two S-matrices (4.17) must solve one of the equations

$$Y_1'(\theta_\nu) = -1, \quad Y_3'(\theta_\nu) = -1 \quad (5.8)$$

depending on value of C'. In addition we shall use the convention that, after crossing the contour, θ_1 has positive imaginary part while θ_2 has negative imaginary part. For $\phi = 0$ we have $\theta_1 = -\theta_2$.

In the leading approximation for large values of the mass parameter m, the non-linear integral equations simplify,

$$\log Y_2'(\theta) = -m'\sqrt{2}\cosh(\theta - i\phi') - \log S_2(\theta - \theta_1) + \log S_2(\theta - \theta_2),$$

$$\log Y_{2\pm1}'(\theta) = -m'\cosh(\theta - i\phi') \pm C' - \log S_1(\theta - \theta_1) + \log S_1(\theta - \theta_2). \quad (5.9)$$

As we explained earlier, the solutions to eq. (5.8) are determined by the poles of the S-matrix, at least to leading order in large m. Since S_2 has poles at θ_S with $\exp i\theta_S = i$, the solutions $\theta_\nu \sim \theta_S/2$ are well approximated by

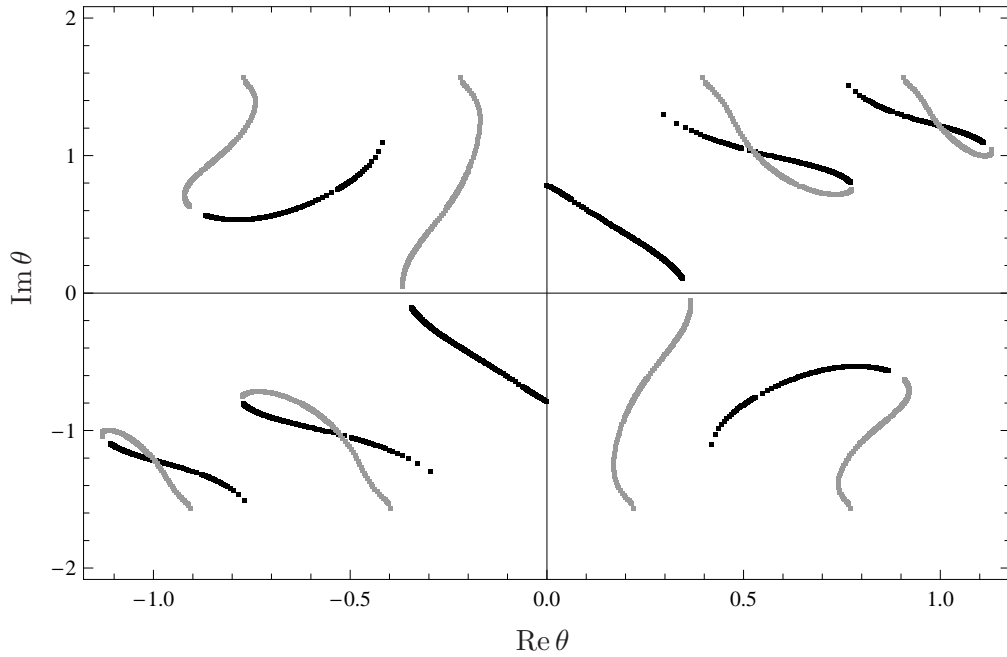$$\theta_1 = -\theta_2 = i\tfrac{\pi}{4} + \dots, \quad (5.10)$$

Figure 4. Positions of some central solutions to the equation $Y_3(\theta) = -1$ along the path depicted in figs. 2, 3. Light dots correspond to positions in the first half of the path before any solution has crossed the real axis while the dark ones are associated with the second part.
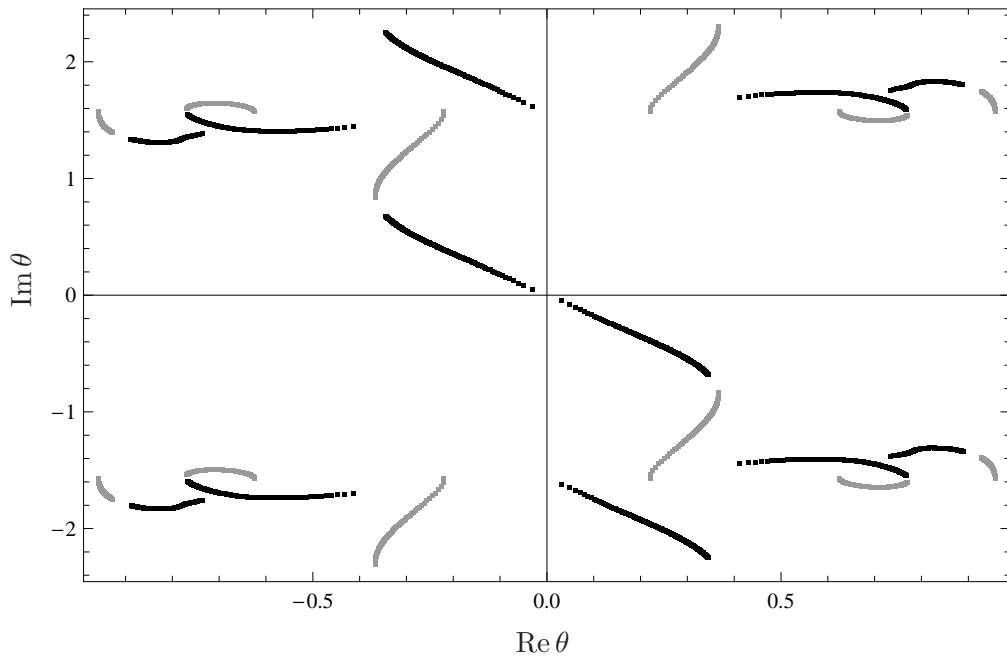

Figure 5. Positions of some central solutions to the equation $Y_2(\theta) = -1$ along the path depicted in figs. 2, 3. We change from light to dark dots at the point where the first solutions of $Y_3 = -1$ cross the real axis.

with corrections of order $\exp(-m)$. We can insert the formulas for Y_i' with $\theta_1 = -\theta_2 = i\pi/4$ into the equations (5.1) and (5.3) that determine the conformal cross ratios u_i' at the endpoint of the analytic continuation. A short computation gives

$$
\begin{aligned}
u_1' &= w'\gamma\varepsilon' + O\left((\varepsilon')^2\right) , \\
u_2' &= (w')^{-1}\gamma\varepsilon' + O\left((\varepsilon')^2\right) , \\
u_3' &= 1 - \left(w' - 2c' + (w')^{-1}\right)\gamma\varepsilon' + O\left((\varepsilon')^2\right) ,
\end{aligned}
\tag{5.11}
$$

with $\gamma = -(3 + 2\sqrt{2})$. Here, the parameters w', c' and ε' are determined by our formulas (3.15) only that we have to replace m, ϕ, C by m', ϕ', C'. At the end of the analytic continuation we want to return to the original values of the cross rations, i.e. we need to impose $u_i = u_i'$. This leads to

$$
\varepsilon' = \gamma^{-1}\varepsilon + O\left(\varepsilon^2\right) , \quad w' = w + O\left(\varepsilon\right) , \quad c' = -c + O\left(\varepsilon\right) ,
\tag{5.12}
$$

Obviously, there exists a second solution of the conditions $u_i = u_i'$. This solution, however, violates the condition $c = -c'$ that we have argued for in the previous subsection.

It is instructive to re-express our relations (5.12) through the parameters m, C and ϕ. We have seen already that $\cosh C' = -\cosh C$. For the other two parameters we obtain

$$
m' = \sqrt{m^2 + s_h^2 + 2ms_h \cos\phi} + O\left(\mathrm{e}^{-m}\right) ,
\tag{5.13}
$$

$$
m'\cos\phi' = s_h + m\cos\phi + O\left(\mathrm{e}^{-m}\right) ,
\tag{5.14}
$$

where $s_h = \log\gamma = -i\pi + \log(3 + 2\sqrt{2})$. Let us recall that these relations between the value of m, C and ϕ in the initial and final point of our curve $\mathcal{C}$ were derived under the assumption of single pole crossing. The numeric results we displayed in the previous section were obtained for $\phi = 0$. In this case, the assumption of single pole crossing gives $\phi' = 0$ and

$$
m' = m - i\pi + \log(3 + 2\sqrt{2})) + O\left(\mathrm{e}^{-m}\right) .
\tag{5.15}
$$

This coincides with the shift we found in our numerical studies, see fig. 2, and provides indirect evidence for the assumption made in the analytic treatment.

Let us now turn to the main goal, namely to the calculation of the remainder function

$$
-R'^{(6)} = A_{\mathrm{free}}'^{(6)} + A_{\mathrm{period}}'^{(6)} - \Delta'^{(6)} + \text{constant} ,
\tag{5.16}
$$

where the individual terms are not evaluated after analytic continuation along the curve $\mathcal{C}$. Let us begin with the function Δ' that was spelled out in eq. (3.4). Upon continuation along the curve (2.11) we find

$$
\begin{aligned}
\Delta'^{(6)} &= \Delta^{(6)} - \tfrac{\pi i}{2}(\log u_3 - \log(1 - u_3)) - \tfrac{\pi^2}{2} \\
&= \tfrac{i}{2}\pi \log\varepsilon + \tfrac{1}{2}i\pi \log\left(2c + w + w^{-1}\right) - \frac{\pi^2}{2} + \Delta^{(6)} + O\left(\varepsilon\right) .
\end{aligned}
\tag{5.17}
$$

In passing from the first to the second line we have inserted the asymptotic form (5.11) of the cross ratios $u_i' = u_i$. The period contribution is even easier to find,

$$A_{\text{period}}^{\prime(6)} = \tfrac{1}{4}(m')^2 = \tfrac{1}{4}(m')^2 - \tfrac{1}{4}(m)^2 + A_{\text{period}}^{(6)}$$

$$= -\frac{1}{2}\log\gamma\,\log(\varepsilon) + \frac{1}{4}\log^2\gamma + A_{\text{period}}^{(6)} + O\left(\varepsilon\right)$$

$$= \tfrac{i}{2}\pi\log(\varepsilon) - \frac{1}{2}\log|\gamma|\,\log(\varepsilon) + \frac{1}{4}\log^2\gamma + A_{\text{period}}^{(6)} + O\left(\varepsilon\right). \qquad (5.18)$$

Finally, we also have to determine the contribution from the free energy. Specializing our general result (4.24) to the present case we find that

$$A_{\text{free}}^{\prime(6)} = \int \frac{d\theta}{2\pi} m' \cosh\theta \log\left[(1 + Y_1'(\theta + i\phi'))(1 + Y_3'(\theta + i\phi'))(1 + Y_2'(\theta + i\phi'))^{\sqrt{2}}\right]$$

$$- m'i\sinh(\theta_1 - i\phi') + m'i\sinh(\theta_2 - i\phi') + \sqrt{2}m'\sinh(|\phi'|). \quad (5.19)$$

Note that the second line contains a contribution from one solution of the equation $Y_2 = -1$. As we explained at the end of section 4.2, the contributions to the free energy arise from solutions θ_* that cross the line $\text{Im}\,\theta_* = \phi$. As one can read off from fig. 5, one of the solutions of $Y_2 = -1$ does cross this line, at least when $\phi \neq 0$.

In the limit of large m, the integral in eq. (5.19) gives a vanishing contribution as one may see by repeating the analysis we have carried out in great detail in section 3.2. So the only terms that are relevant in the Regge limit come from the second line of the previous equation. This gives

$$A_{\text{free}}^{\prime(6)} = \sqrt{2}m'\cos(\phi') + \sqrt{2}m'\sinh(|\phi'|) + O\left(\varepsilon\right) = \sqrt{2}\log\varepsilon' + \sqrt{2}|\log w'| + O\left(\varepsilon\right)$$

$$= -\sqrt{2}\log\varepsilon + \sqrt{2}\log\gamma + A_{\text{free}}^{(6)} + \sqrt{2}|\log w| + O\left(\varepsilon\right). \qquad (5.20)$$

In passing to lower line, we have inserted eq. (5.14) and also added the term A_{free} that was evaluated in section 3.2. Since the free energy before analytic continuation vanishes in the limit of $\varepsilon \to 0$, the additional term is actually zero. We only put it back in to show that the leading term should be regarded as a difference of energies. Using the final result (3.25) of our computation in section 3.2, we are now prepared to determine the Regge limit of the remainder function in the regime (2.8),

$$-R^{\prime(6)} = A_{\text{free}}^{\prime(6)} + A_{\text{period}}^{\prime(6)} - \Delta^{\prime(6)}$$

$$= -e_2\log\varepsilon - \tfrac{\pi}{2}i\log\left(2c + w + w^{-1}\right) + \sqrt{2}|\log w| + \text{constant}' + O\left(\varepsilon\right). (5.21)$$

Here, we have moved all the constant terms into a redefinition of the 'constant' and defined the constant e_2 by

$$e_2 = \left(\sqrt{2} + \tfrac{1}{2}\log(3 + 2\sqrt{2})\right). \qquad (5.22)$$

In a final step, we want to express the variables w, c and ε through the conformal cross ratios. Using eqs. (3.17) along with

$$\varepsilon = \sqrt{\tilde{u}_1\tilde{u}_2}(1 - u_3), \qquad (5.23)$$

we find that

$$-R' = -e_2 \log((1-u_3)\sqrt{\tilde{u}_1\tilde{u}_2}) + \tfrac{1}{2}i\pi \log \sqrt{\tilde{u}_1\tilde{u}_2} + \sqrt{2}|\log(\tilde{u}_1/\tilde{u}_2)|$$
$$+\text{const}' + O\left(1 - \tilde{u}_3\right) . \tag{5.24}$$

After exponentiation of this result we obtain

$$\text{Amp}' \sim \langle W' \rangle \sim \exp\left[-\frac{\sqrt{\lambda}}{2\pi}A'\right] = \exp\left[-\frac{\sqrt{\lambda}}{2\pi}(A'_{\text{div}} + A'_{\text{BDS}} - R')\right] , \tag{5.25}$$

with

$$e^{\frac{\sqrt{\lambda}}{2\pi}R'} \sim e^{-i\frac{\pi}{2}\frac{\sqrt{\lambda}}{4\pi}\ln(\tilde{u}_1\tilde{u}_2)}\left((1-u_3)\sqrt{\tilde{u}_1\tilde{u}_2}\right)^{\frac{\sqrt{\lambda}}{2\pi}e_2}$$
$$\times\left[\left(\frac{\tilde{u}_1}{\tilde{u}_2}\right)^{-\frac{\sqrt{\lambda}}{\sqrt{2}\pi}}\theta\left(\frac{\tilde{u}_1}{\tilde{u}_2}-1\right) + \left(\frac{\tilde{u}_2}{\tilde{u}_1}\right)^{-\frac{\sqrt{\lambda}}{\sqrt{2}\pi}}\theta\left(\frac{\tilde{u}_2}{\tilde{u}_1}-1\right)\right] , \tag{5.26}$$

up to some irrelevant constant prefactor. This formula is the main result of our analysis. It describes the Regge limit of the six-gluon amplitude in the mixed regime and at strong coupling. As we have stressed before, our calculation assumes that the analytical continuation of the amplitude may be performed within the prescription of Alday et al., see our discussion in the introduction and the next section.

Before we conclude, we would like to compare our result with the form of the answer at weak coupling. The relevant expression is known in the leading logarithmic approximation [19]. The following formula gives the correction to the BDS expression:

$$\text{Amp}' = \text{Amp}_{2\to4}^{BDS}\ (1 + i\Delta_{2\to4}) , \tag{5.27}$$

with

$$\Delta_{2\to4} = \frac{a}{2}\sum_{n=-\infty}^{n=\infty}(-1)^n\int\frac{d\nu}{\nu^2 + \frac{n^2}{4}}(s_2^{\omega(\nu,n)} - 1)\left(\frac{q_2^*p_4^*}{p_5^*q_1^*}\right)^{i\nu-\frac{n}{2}}\left(\frac{q_2p_4}{p_5q_1}\right)^{i\nu+\frac{n}{2}} . \tag{5.28}$$

All relevant notations are explained in [19]. In particular, the q_i are the transverse momenta of the t_i invariants, the parameter a is given by $a = \lambda/8\pi^2$ and λ is the 't Hooft coupling $\lambda = g^2N_c$. The exponent ω of s_2 is given by

$$\omega(\nu,n) = 4a\mathcal{R}\left(2\psi(1) - \psi(1 + i\nu + \frac{n}{2}) - \psi(1 + i\nu - \frac{n}{2})\right) . \tag{5.29}$$

In the weak coupling expression (5.27) the new term, $\Delta_{2\to4}$, comes as an additive correction. There is no indication that this correction should be written as an exponential. From the point of view of Regge theory, it seems more natural to sum over the different singularities in the complex angular momentum plane, and it is not clear whether exponentiation would still be consistent with Regge factorization. However, the leading logarithmic approximation alone is not sufficient to exclude the possibility of exponentiation.

The function $\Delta_{2\to4}$ may be re-expressed in terms of the cross ratios u_i that we have built in section 2. In these variables, (5.28) assumes the form

$$\Delta_{2\to4} = \frac{a}{2}\sum_{n=0}^{n=\infty}(-1)^n\int\frac{d\nu}{\nu^2+\frac{n^2}{4}}((1-u_3)^{-\omega(\nu,n)}-1)\left(\frac{\tilde{u}_1}{\tilde{u}_2}\right)^{i\nu}\cosh nC\,,\qquad(5.30)$$

where we have used $1-u_3\sim 1/s_2$ (appendix A),

$$\left|\frac{q_2p_4}{p_5q_1}\right|=\sqrt{\frac{\tilde{u}_1}{\tilde{u}_2}}\approx w\,,\qquad(5.31)$$

and

$$\cos\left(\arg\frac{q_2p_4}{p_5q_1}\right)=\frac{1-u_1-u_2-u_3}{2\sqrt{u_1u_2}}\approx\frac{1-u_1-u_2-u_3}{2\sqrt{u_1u_2u_3}}=\cosh C.\qquad(5.32)$$

The leading power of s_2 belongs to $n=1$ and $\nu=0$ so that the intercept at weak coupling becomes

$$\omega(0,1) = -E_2 = \frac{\lambda}{\pi^2}(2\ln 2-1)\,.\qquad(5.33)$$

Consequently, up to logarithmic corrections, the leading asymptotic behavior of the remainder function at weak coupling is given by

$$\Delta_{2\to4} \sim \frac{a}{2}(1-u_3)^{-\omega(0,1)}\ \cosh C\,.\qquad(5.34)$$

In this leading logarithmic approximation, it is not possible to determine the scale of the energy s_2. Put differently, the factor $1-u_3$ may be accompanied by some undetermined finite function of $\tilde{u}_1$ and $\tilde{u}_2$.

Let us attempt a first comparison of our strong coupling result eq. (5.26) with the weak coupling amplitude in eqs. (5.27),(5.28) and eq. (5.34). In both cases, the energy dependence of the correction is power-behaved (i.e. Regge-behaved). We first face the fact that, at weak coupling, the correction is additive whereas, at strong coupling, the remainder function in the exponent leads to a multiplicative correction to the BDS amplitude. As a possible interpretation, we might assume that in eq. (5.27) the correction, which at weak coupling is of order λ, grows with λ and, at strong coupling, dominates over the 1. We are then led to confront $\Delta_{2\to4}$ in eqs. (5.30) and (5.34) with eq. (5.26).

A striking observation is the change in the sign of the exponent E_2: The intercept of the energy s_2 which on the weak coupling side is positive appears to turn negative when the coupling is increased. Also, the strong coupling expression exhibits an energy scale depending upon the product of $\tilde{u}_1$ and $\tilde{u}_2$. Next let us look at the ratio $\tilde{u}_1/\tilde{u}_2$ which is raised to power $i\nu$ on the weak coupling side. Since at large s_2 the leading behavior comes from $i\nu=0$, the dependence on $\tilde{u}_1/\tilde{u}_2$ drops out of eq. (5.34). In contrast to this, on the strong coupling side, the ratio $\tilde{u}_1/\tilde{u}_2$ comes with an exponent of order $\sqrt{\lambda}$. In addition, the factor $\cosh C$ that multiplies the answer at weak coupling, is absent at strong coupling. Finally, in eq. (5.26), we see a phase factor which also depends upon the product of $\tilde{u}_1$ and

$\tilde{u}_2$. It should be kept in mind, however, that the full BDS amplitude at strong coupling, $A_{\text{div}}^{(6)} + A_{\text{BDS}}^{(6)}$, when continued into the mixed region, also contains a phase: A straightforward calculation shows that this phase exactly cancels the phase in eq. (5.26). As a result, the strong coupling result has no such phase factor.[3]

Let us try a further interpretation and assume that, at strong coupling, the correction factor $\exp(\sqrt{\lambda} R'/2\pi)$ can also be written in the form of eq. (5.30) as an expansion in the two-dimensional conformal group (Möbius group), with some strong coupling analogue $\tilde{\omega}(\nu, n)$ of the function $\omega(\nu, n)$. Then, in eq. (5.26), the exponent of $\tilde{u}_1/\tilde{u}_2$ could be interpreted as coming from a dominant ν-value ν_s that is of the order $\sqrt{\lambda}$. At the same time, the exponent of s_2 would come from the function $\tilde{\omega}(\nu, n)$, evaluated at the value ν_s. Finally, the absence of the factor $\cosh C$ might result from the fact that, at large ν_s, $\tilde{\omega}(\nu_s, 0)$ dominates over $\tilde{\omega}(\nu_s, 1)$. In pursuing such an interpretation one would perform a saddle point analysis of the ν-integral: At weak coupling, the large parameter is $\ln s_2$ which leads to the dominance of the point $\nu = 0$. In contrast, at strong coupling it is $\sqrt{\lambda}$ which plays the role of the large parameter, leading to a value $\nu_2 = \mathcal{O}(\sqrt{\lambda})$. In this sense, the form of our strong coupling results seems perfectly consistent with the general features of Regge theory.

6 Conclusions and Outlook

In this paper we have studied the Regge limit of the planar six-point function at strong coupling. In the weak coupling regime this high energy limit, taken in a very special kinematic region ('mixed region') where some energies are positive while others are negative, is known to be particularly sensitive to the analytic properties of scattering amplitudes. Making use of the set of equations for Y-functions, we have been able to perform the analytic continuation of the scattering amplitude at strong coupling into this kinematic region and to calculate new corrections which are given by excitations of the auxiliary quantum integrable system. A comparison of the strong coupling result with the expressions for weak coupling shows interesting features but needs further investigations. At the moment, nothing is known about how the quantity E_2 may be interpolated between weak and strong coupling.

As we pointed out in the introduction, our calculation of the parameter E_2 at strong coupling was based on one important assumption, namely that we can simply continue the prescription of Alday et al. into the mixed regime. In other words, we have assumed that the amplitude in the mixed regime is determined by the exponential of the free energy in the auxiliary quantum integrable system. One may certainly wonder whether this assumption was justified. As we sketched in the introduction, scattering amplitudes at strong coupling do possess a geometric origin. According to the original prescription of Alday and Maldacena, they are determined by the area of a 2-dimensional surface S_6 which stretches to the boundary of AdS_5. This surface emerges as the unique saddle point that dominates the string theoretic path integral in the limit of strong 't Hooft coupling. The kinematic invariants of the scattering process are encoded in the shape of the 1-dimensional boundary

---

[3] In the weak coupling regime, it was the appearance of such a phase factor in the BDS amplitude which played a vital role in understanding the deficiency of the BDS formula. The complete cancellation of the phases at strong coupling therefore provides support for the correct analytic structure at strong coupling.

∂S_6 of S_6 in the boundary of AdS_5. Our analytic continuation in the space of kinematic invariants amounts to a continuation in the boundary conditions for a (path) integral. In any saddle point approximation, the contributing saddle points can be very sensitive to boundary conditions. In fact, there could even exist points, i.e. values of the kinematic invariants in our case, at which several saddle points contribute to the same order. From this point of view it seems far from obvious that amplitudes in the mixed regime can be obtained by simple analytic continuation and that they contain a single exponential term. This issue certainly deserves further investigation.

There are a few more or less obvious extensions of this work. It seems worthwhile exploring the relation between the analytic structure of scattering amplitudes and excited states of the auxiliary quantum system for more general cases, including other regimes and for a larger number of external gluons. In this context it might be useful to work with an alternative version of the non-linear integrable equations [32] in which only the geometric cross ratios appear as fundamental parameters.[4] Another question addresses the relation between excited states and analytic continuation. For other quantum integrable systems it is well-known that there exist excited states that are not related to analytic continuation in the parameters. The associated integral equations are of the same form, but without any constraints in the numbers N of driving terms. One may wonder whether such excited states could also have some interpretation in the context of scattering amplitudes.

A   Kinematics in the Regge limit

In this appendix we shall analyze the behavior of the conformal cross ratios u_i in the ordinary multi-Regge limit

$$s \gg s_1, s_2, s_3 \gg -t_1, -t_2 \sim 1. \tag{A.1}$$

When written in light-cone coordinates, the asymptotical behavior of our six momentum vectors $p_3 = (p_i^+, p_i^-, p_i^2, p_i^3)$ may be parametrized by

$$p_1 \sim (-\omega^{-1}, -\omega, \dots) \quad , \quad p_2 \sim (-\omega, -\omega^{-1}, \dots),$$
$$p_3 \sim (\omega, \omega^{-1}, \dots) \quad , \quad p_4 \sim (\omega^a, \omega^{-a}, \dots),$$
$$p_5 \sim (\omega^{-b}, \omega^b, \dots) \quad , \quad p_6 \sim (\omega^{-1}, \omega, \dots),$$

where ω is a parameter that becomes large in the Regge limit and we have only displayed the leading terms in the limit $\omega \to \infty$. The two exponents a,b are free finite parameters.

---

[4]Since the contribution $A^{(6)}_{\text{period}}$ is most easily expressed in terms of the variable m, however, one must still determine this parameter as a function of the cross ratios u_i.

Note that all transverse momenta must be finite to satisfy the on-shell condition. The dependence of kinematic invariants on ω is now easy to compute

$$s \sim \omega^2 \quad, \qquad s_{456} \sim \omega^{(1+a)} \quad, \qquad s_{345} \sim \omega^{(1+b)} \,,$$

$$s_1 \sim \omega^{(1-a)} \quad, \qquad s_2 \sim \omega^{(a+b)} \quad, \qquad s_3 \sim \omega^{(1-b)} \,,$$

$$-t_1 \sim \omega^0 \quad, \qquad -t_2 \sim \omega^0 \quad, \qquad -s_{234} \sim \omega^0 \,.$$

Depending on our choice of a and b we can realize various asymptotics of the kinematic invariants. If $a = b = 1$, for example, one finds $s_2 \sim s$. A regime with $s_1 \sim s_2 \sim s_3$ is reached in case we set $a = b = 1/3$. Setting $a = b = 0$, on the other hand, allows us to perform a quasi multi-Regge limit in which $s_2 \sim 1$.

From the scaling properties of kinematic invariants we can easily deduce the following behavior of the cross-ratios (2.4),

$$u_1 \sim \omega^{-(a+b)} \sim s_2^{-1} \quad, \quad u_2 \sim \omega^{-(a+b)} \sim s_2^{-1} \,. \tag{A.2}$$

Thereby we have shown that u_1 and u_2 vanish at the same order when we take our Regge limit. Their ratio u_1/u_2 remains constant. It remains to study the properties of u_3. Using the Gram determinant relation to express s in terms of the other eight kinematic invariants we find

$$u_3 = \frac{s_2 s}{s_{456} s_{345}} = 1 - f(s_i, t_i, s_{i,i+1,i+2}) \,. \tag{A.3}$$

After substitution of the gluon momenta we obtain

$$f(s_i, t_i, s_{i,i+1,i+2}) \sim \omega^{-(a+b)} \sim s_2^{-1} \,. \tag{A.4}$$

Hence, both $u_1/(1-u_3)$ and $u_2/(1-u_3)$ remain finite for $\omega \to \infty$. We have used these two ratios to parametrize amplitudes in the Regge limit.

B Hirota equations

There exists another important set of functions $T_{s,m}$ that appear in the context of gluon scattering. Our discussion in this appendix will be kept general, i.e. it applies to an arbitrary number n of gluons. The functions $T_{s,m} = T_{s,m}(\theta)$ are parametrized by two integers s, m. They are subject to the following set of Hirota equations,

$$T_{s,m}^+ T_{4-s,m}^- = T_{4-s,m+1} T_{s,m-1} + T_{s+1,m} T_{s-1,m} \,, \tag{B.1}$$

for $s = 1, 2, 3$. The superscipts $\pm$ indicate shifts of the spectral parameter, i.e.

$$f^\pm(\theta) = f^{[\pm 1]}(\theta) \quad \text{with} \quad f^{[m]}(\theta) = f(\theta + im\tfrac{\pi}{4}) \,.$$

We complete the description of the functions $T_{s,m}$ by a list of boundary conditions.

$$T_{s,-1} = T_{s,n-4} = 0 \,, \quad \text{where} \quad s = 1, 2, 3 \tag{B.2}$$

and

$$T_{s,0} \; = \; T_{0,m} \; = \; T_{4,m} \; = \; 1 \; . \tag{B.3}$$

Here, n is the number of gluons. After imposing boundary conditions, we are left with $3(n-5)$ functions.

The $T_{s,m}$ are related to $Y_{s,m}$ we have used throughout our discussion through the relations

$$Y_{s,m} \; \equiv \; \frac{T_{s,m+1}T_{4-s,m-1}}{T_{s+1,m}T_{s-1,m}} \; . \tag{B.4}$$

Inserting these into the Hirota equations (B.1) we obtain

$$\frac{Y_{s,m}^{-}Y_{4-s,m}^{+}}{Y_{s+1,m}Y_{s-1,m}} \; = \; \frac{(1+Y_{s,m+1})(1+Y_{4-s,m-1})}{(1+Y_{s+1,m})(1+Y_{s-1,m})} \; , \tag{B.5}$$

where $s = 1,2,3$ and $m = 1,2,\ldots,n-5$. The behavior of $T_{s,m}$ on the boundary translate into the following boundary conditions for $Y_{s,m}$,

$$Y_{0,m} \; = \; Y_{4,m} = \infty \, , \quad \text{and} \quad Y_{s,0} \; = \; Y_{s,n-4} = 0 \quad \text{with} \quad s = 1,2,3 \; . \tag{B.6}$$

Using the set of $Y-$functions one may relate the parameters m_m, ϕ_m, C_m of the $Y-$system through cross ratios. In order to do so, one has to invert the following relations

$$\frac{x_{p-k-1,p+k}^{2}x_{p-k-2,p+k-1}^{2}}{x_{p-k-2,p+k}^{2}x_{p-k-1,p+k-1}^{2}} \; = \; \left(1+\frac{1}{Y_{2,2k-1}}\right)_{\theta=\frac{i\pi}{4}(2p-1)} \; = \; \left(\frac{T_{2,2k-1}^{+}T_{2,2k-1}^{-}}{T_{2,2k}T_{2,2k-3}}\right)_{\theta=\frac{i\pi}{4}(2p-1)} \; . \tag{B.7}$$

Our equations (3.8) are recovered as a special case when $n = 6$ with $k = 1$ and $p = -1,0,1$. We have pointed out before that the Y-functions satisfy the usual non-linear equations as long as their argument θ remains inside the strip $|\operatorname{Im}(\theta)| \leq \pi/4$. Whenever θ crosses one of the lines $\operatorname{Im}(\theta) = ir\pi/4$, one has to add contributions from poles of the kernel functions K_i. To avoid these complications, we can also solve the original equations inside the fundamental strip and extend the solutions to the complex plane recursively, with the help of the $Y-$system equation, i.e.

$$Y_{s,m} \; = \; \frac{(1+Y_{s,m+1}^{[1]})(1+Y_{4-s,m-1}^{[1]})}{Y_{4-s,m}^{[2]}(1+1/Y_{s+1,m}^{[1]})(1+1/Y_{s-1,m}^{[1]})} \; . \tag{B.8}$$

We have used this recursive construction of $Y_s = Y_{s,1}$ is section 3.1 to obtain the formula (3.9) for the cross ratio u_3.

C Comments on numerical computations

In this work, numerical calculations were used to find the path of the analytical continuation in the space of parameters m, ϕ, C and to check which solutions of $Y_i = -1$ cross the integration contour. Most of this was done with the help of Mathematica.

In order to determine the $Y-$functions for fixed m, ϕ and C we use an algorithm similar to one presented in [29] for the case of AdS_3. It involves solving the non-linear integral

equations (3.5) and (3.6) perturbatively for large enough m. The leading solution is given by expressions that do not contain integrals, namely our eqs. (3.12) and (3.13). To obtain the solution with better precision we insert the kth iteration into the integrals to obtain, i.e. schematically

$$\log Y_i^{(k+1)}(\theta) \;=\; -m_i \cosh(\theta - i\phi) + C_i + (K_{ij} \star \log(1 + Y_i^{(k)}))(\theta)\,. \qquad \text{(C.1)}$$

We perform k such iterations until the Y−functions stabilize. As a result we obtain Y−functions of real θ, or rather a discrete subset thereof. Moreover, using the integral equations we can calculate the Y−functions for complex value of θ by convoluting the kernel functions K_i with the Y−functions of real θ. Due to existence of the poles in the kernels, we must limit this evaluation of the Y-functions in the complex θ-plane to the strip $|\operatorname{Im}\theta| < \frac{\pi}{4}$. For values of θ outside this strip, we recursively use Hirota equations (B.8). In this way, we can construct Y−functions on the whole complex θ−plane.

Next, we evaluate the Y−functions for special values of $\theta = \pm\pi i/4, 3\pi i/4$ which determine the cross ratios u_i defined in eq. (3.8). Actually, for these values of θ the numerical algorithms are not well convergent and it is easier at these points to interpolate the Y−functions. But at the end one can relate values of m, ϕ and C to values u_i. In order to find Y−functions along our analytical continuations contour defined by eq. (2.11) one has to invert the relation between the parameters m, ϕ and C and the cross ratios u_i. The values of C along the path can be found analytically, namely it is given by eq. (5.3). The other two parameters m and ϕ, on the other hand, require numerical calculations. An example of such path is shown in figs. 2,3. Here, it has been performed by solving a set of nonlinear equations (3.8) using the Newton method.

Furthermore, one can also determine the positions of solutions to the equations $Y_i = -1$ numerically, see figs. 4,5. These solutions are moving while we are continuing along the contour in parameter space. In the process of this continuation, some solutions of $Y_3 = -1$ and $Y_1 = -1$ cross the real line. This happens roughly when $\varphi \sim \pi/2$. At this point we must replace the original non-linear equations by those spelled out in eqs. (5.4) and (5.5).

The numerical results show that during analytical continuations only from of the solutions to $Y_i = -1$ cross the integral contour, see figs. 4 and 5. Moreover, to a very good approximation, the imaginary parts of m and ϕ behave linearly with φ while their real parts change quadratically, compare also fig. 2. At the end of the contour path, m and ϕ go to values which are captured by our eqs. (5.13) and (5.14).

References

[1] A. M. Polyakov, *Gauge Fields as Rings of Glue*, Nucl. Phys. **B164** (1980) 171–188.

[2] J. M. Maldacena, *The large N limit of superconformal field theories and supergravity*, Adv. Theor. Math. Phys. **2** (1998) 231–252, [hep-th/9711200].

[3] E. Witten, *Anti-de Sitter space and holography*, Adv. Theor. Math. Phys. **2** (1998) 253–291, [hep-th/9802150].

[4] S. S. Gubser, I. R. Klebanov, and A. M. Polyakov, *Gauge theory correlators from non-critical string theory*, Phys. Lett. **B428** (1998) 105–114, [hep-th/9802109].

[5] G. Arutyunov and S. Frolov, *String hypothesis for the $AdS_5 \times S^5$ mirror*, *JHEP* **03** (2009) 152, [arXiv:0901.1417].

[6] N. Gromov, V. Kazakov, and P. Vieira, *Exact Spectrum of Anomalous Dimensions of Planar N=4 Supersymmetric Yang-Mills Theory*, *Phys. Rev. Lett.* **103** (2009) 131601, [arXiv:0901.3753].

[7] D. Bombardelli, D. Fioravanti, and R. Tateo, *Thermodynamic Bethe Ansatz for planar AdS/CFT: a proposal*, *J. Phys.* **A42** (2009) 375401, [arXiv:0902.3930].

[8] N. Gromov, V. Kazakov, A. Kozak, and P. Vieira, *Exact Spectrum of Anomalous Dimensions of Planar N = 4 Supersymmetric Yang-Mills Theory: TBA and excited states*, *Lett. Math. Phys.* **91** (2010) 265–287, [arXiv:0902.4458].

[9] G. Arutyunov and S. Frolov, *Thermodynamic Bethe Ansatz for the $AdS_5 \times S^5$ Mirror Model*, *JHEP* **05** (2009) 068, [arXiv:0903.0141].

[10] A. Hegedus, *Discrete Hirota dynamics for AdS/CFT*, *Nucl. Phys.* **B825** (2010) 341–365, [arXiv:0906.2546].

[11] N. Gromov, V. Kazakov, and P. Vieira, *Exact Spectrum of Planar $\mathcal{N} = 4$ Supersymmetric Yang- Mills Theory: Konishi Dimension at Any Coupling*, *Phys. Rev. Lett.* **104** (2010) 211601, [arXiv:0906.4240].

[12] G. Arutyunov and S. Frolov, *Simplified TBA equations of the $AdS_5 \times S^5$ mirror model*, *JHEP* **11** (2009) 019, [arXiv:0907.2647].

[13] N. Gromov, *Y-system and Quasi-Classical Strings*, *JHEP* **01** (2010) 112, [arXiv:0910.3608].

[14] Z. Bern, L. J. Dixon, and V. A. Smirnov, *Iteration of planar amplitudes in maximally supersymmetric Yang-Mills theory at three loops and beyond*, *Phys. Rev.* **D72** (2005) 085001, [hep-th/0505205].

[15] J. M. Drummond, J. Henn, G. P. Korchemsky, and E. Sokatchev, *Conformal Ward identities for Wilson loops and a test of the duality with gluon amplitudes*, *Nucl. Phys.* **B826** (2010) 337–364, [arXiv:0712.1223].

[16] J. M. Drummond, J. Henn, G. P. Korchemsky, and E. Sokatchev, *The hexagon Wilson loop and the BDS ansatz for the six- gluon amplitude*, *Phys. Lett.* **B662** (2008) 456–460, [arXiv:0712.4138].

[17] Z. Bern *et. al.*, *The Two-Loop Six-Gluon MHV Amplitude in Maximally Supersymmetric Yang-Mills Theory*, *Phys. Rev.* **D78** (2008) 045007, [arXiv:0803.1465].

[18] J. Bartels, L. N. Lipatov, and A. Sabio Vera, *BFKL Pomeron, Reggeized gluons and Bern-Dixon-Smirnov amplitudes*, *Phys. Rev.* **D80** (2009) 045002, [arXiv:0802.2065].

[19] J. Bartels, L. N. Lipatov, and A. Sabio Vera, *N=4 supersymmetric Yang Mills scattering amplitudes at high energies: the Regge cut contribution*, *Eur. Phys. J.* **C65** (2010) 587–605, [arXiv:0807.0894].

[20] R. M. Schabinger, *The Imaginary Part of the N = 4 Super-Yang-Mills Two-Loop Six-Point MHV Amplitude in Multi-Regge Kinematics*, *JHEP* **11** (2009) 108, [arXiv:0910.3933].

[21] L. N. Lipatov and A. Prygarin, *Mandelstam cuts and light-like Wilson loops in N=4 SUSY*, arXiv:1008.1016.

[22] A. B. Goncharov, M. Spradlin, C. Vergu, and A. Volovich, *Classical Polylogarithms for Amplitudes and Wilson Loops*, arXiv:1006.5703.

[23] V. Del Duca, C. Duhr, and V. A. Smirnov, *An Analytic Result for the Two-Loop Hexagon Wilson Loop in N = 4 SYM*, *JHEP* **03** (2010) 099, [arXiv:0911.5332].

[24] V. Del Duca, C. Duhr, and V. A. Smirnov, *The Two-Loop Hexagon Wilson Loop in N = 4 SYM*, *JHEP* **05** (2010) 084, [arXiv:1003.1702].

[25] L. N. Lipatov, *Integrability of scattering amplitudes in N=4 SUSY*, *J. Phys.* **A42** (2009) 304020, [arXiv:0902.1444].

[26] L. F. Alday and J. M. Maldacena, *Gluon scattering amplitudes at strong coupling*, *JHEP* **06** (2007) 064, [arXiv:0705.0303].

[27] L. F. Alday and J. Maldacena, *Null polygonal Wilson loops and minimal surfaces in Anti-de-Sitter space*, *JHEP* **11** (2009) 082, [arXiv:0904.0663].

[28] L. F. Alday, D. Gaiotto, and J. Maldacena, *Thermodynamic Bubble Ansatz*, arXiv:0911.4708.

[29] L. F. Alday, J. Maldacena, A. Sever, and P. Vieira, *Y-system for Scattering Amplitudes*, arXiv:1002.2459.

[30] P. Dorey and R. Tateo, *Excited states by analytic continuation of TBA equations*, *Nucl. Phys.* **B482** (1996) 639–659, [hep-th/9607167].

[31] P. Dorey and R. Tateo, *Excited states in some simple perturbed conformal field theories*, *Nucl. Phys.* **B515** (1998) 575–623, [hep-th/9706140].

[32] L. F. Alday, D. Gaiotto, J. Maldacena, A. Sever, and P. Vieira, *An Operator Product Expansion for Polygonal null Wilson Loops*, arXiv:1006.2788.

[33] Y. Hatsuda, K. Ito, K. Sakai, and Y. Satoh, *Six-point gluon scattering amplitudes from Z_4-symmetric integrable model*, *JHEP* **09** (2010) 064, [arXiv:1005.4487].

[34] I. Gradshteyn and I. Ryzhik, *Table of integrals, series, and products. Translated from the Russian. Translation edited and with a preface by Alan Jeffrey and Daniel Zwillinger. 6th ed.* San Diego, CA: Academic Press. xlvii, 1163 p., 2000.